



EARTHQUAKE RESPONSE ANALYSIS OF RC BRIDGE PIERS INCLUDING THE EFFECT OF REPAIR/RETROFITTING

D. H. Lee,¹ S. Yun² and T. Park³

ABSTRACT

For the evaluation of the seismic performance of retrofitted reinforced concrete columns, an inelastic repair element is suggested. The suggested repair element is capable of reflecting the structural intervention (repair or retrofitting) in terms of the direct modelling of the intervention. The repair element, having both birth and death time, can be activated within the user-defined time intervals of interest during both static and dynamic time-history analysis. Comparative evaluation is conducted for reinforced concrete column tests which are repaired and retrofitted. Analytical predictions obtained with the proposed repair element display reasonably good correlation with test results. It is therefore encouraged that the new element can be used for the healthy seismic evaluation of reinforced concrete columns being repaired and retrofitted.

Introduction

One of the most fundamental observations in the past earthquakes is that the earthquakes have random nature and earthquake magnitudes are inversely proportional to their likelihood of occurrence. Structures constructed in seismic zones can thus be expected to undergo numerous earthquakes that may be either greater or lesser intensity prior to being subjected to a design level earthquake. Moreover, those structures may experience successive earthquakes within a certain time interval. For example, following the Kocaeli earthquake on 17 August 1999, another Duzce earthquake on 12 November 1999 (three months later) occurred in the area of Duzce and Bolu, northwestern part of Turkey, which is located in near of Kocaeli (Sucuoglu 2002, Uckan et al. 2002). This implies that the survived lifeline structures such as bridges under the former event may have damage or collapse potential under the latter event. Therefore, it is of utmost importance that seismic analysis of such structures should account for the prior damage effect, particularly when the structures are being repaired or retrofitted after the former event. Otherwise, erroneous response characteristics for such repaired or retrofitted structures can be estimated and thus may prejudice the stability assessment of such structures under the latter event.

In view of the above, to assess the seismic performance of reinforced concrete members being repaired and retrofitted after experiencing prior earthquake damage, repair element is proposed. This repair element having both birth and death time can freely be activated (or deactivated) within the user-defined

¹Associate Professor, Dept. of Civil, Environmental & Railroad Engineering., Paichai University, 439-6 Doma-2 dong, Seo-Gu, Daejeon 302-735, Korea, Email: dohlee@pcu.ac.kr

²PhD Candidate, Dept. of Civil Engineering, Hanyang University, 17 Haengdang-dong, Seoul 133-791, Korea

³Associate Professor, Dept. of Civil Engineering, Hanyang University, 17 Haengdang-dong, Seoul 133-791, Korea

time intervals of interests during static and dynamic time history analysis. In turn, an analysis with the repair element can continually be performed with increased characteristics due to repair or retrofitted measure while degraded strength and stiffness of members (or structures) experienced the initial loading history and prior earthquake for static and dynamic time history analysis, respectively are kept as they are. This allows the repair element to reflect the realistic behavior of such members (or structures) being repaired or retrofitted. Derivation and verification of the element are discussed hereafter.

Repair Element and Program ZeusNL

Derivation of Repair Element

Repair element having both birth and death time is proposed for the assessment of seismic behavior of reinforced concrete members experienced prior damage. The element is derived from the inelastic cubic formulation developed by Izzuddin and Elnashai (1993a, b). The formulation is capable of modeling material inelasticity effects in terms of a detailed consideration of section type and constitutive relationship of the material. In addition, the effect of large displacement is also included in the formulation. Since the formulation contains all the salient features needed for the current development, the inelastic cubic formulation proposed by Izzuddin and Elnashai is thus adopted for the development of the repair element.

Four assumptions are made in the derivation of the cubic formulation, which are 1) warping strains due to nonuniform torsion are ignored, 2) plane sections remain plane, 3) shear strains due to flexure are ignored, and 4) shear center and section centroid are coincident. The above four assumptions allow strain state within a cross section to be determined only by four generalized strains, which are centroidal axial strain, rate of twist, and curvature strains about the two principal axes. The four generalized strains will be discussed hereafter.

Six local degrees of freedom are employed for the three dimensional inelastic cubic formulation as shown in Fig. 1. Local displacement vector $\tilde{\mathbf{u}}_c$ and local force vector $\tilde{\mathbf{f}}_c$ of an element is expressed in terms of the six local degrees of freedom, which is given by,

$$\tilde{\mathbf{u}}_c = \{\theta_{1y}, \theta_{1z}, \theta_{2y}, \theta_{2z}, \Delta, \theta_T\}^T \quad (1)$$

$$\tilde{\mathbf{f}}_c = \{M_{1y}, M_{1z}, M_{2y}, M_{2z}, F, m_T\}^T \quad (2)$$

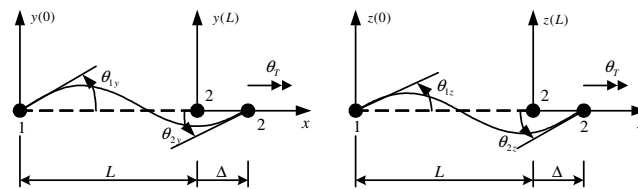


Figure 1. Local freedoms of inelastic cubic formulation.

Since the formulation is intended to represent short lengths of members which can be assumed straight, variables for imperfections are not taken into account. Depicted in Fig. 2 is the movement of a point along the element reference axis. The movement of a point can be described by the shown four displacement values that are defined by interpolation functions given by,

$$\alpha(x) = \theta_T \left(\frac{x}{L} \right) \quad (3)$$

$$v(x) = \left(\frac{\theta_{1y} + \theta_{2y}}{L^2} \right) x^3 - \left(\frac{2\theta_{1y} + \theta_{2y}}{L} \right) x^2 + (\theta_{1y})x \quad (4)$$

$$w(x) = \left(\frac{\theta_{1z} + \theta_{2z}}{L^2} \right) x^3 - \left(\frac{2\theta_{1z} + \theta_{2z}}{L} \right) x^2 + (\theta_{1z})x \quad (5)$$

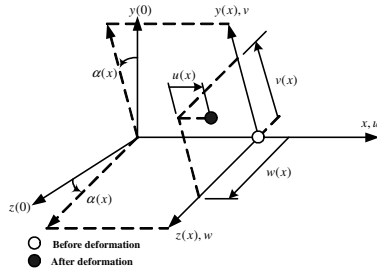


Figure 2. Movement of a point along the element.

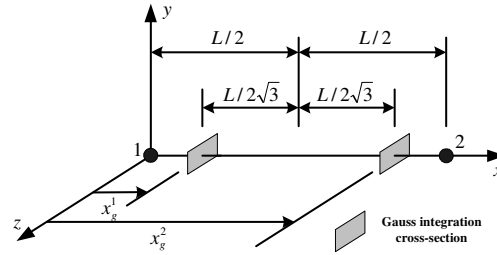


Figure 3. Position of two Gauss integration sections.

Since the centroidal axial strain is assumed constant along the element length, no interpolation function is required for the axial displacement $\mathbf{u}(\mathbf{x})$. This assumption that axial force is constant along the element length may be violated for the presence of material plasticity. However, if the element is used to model short lengths of inelastic members as mentioned above, the axial force variation is insignificant and hence the assumption can be reasonable. The rest three generalized strains are calculated from the assumption of small local deformation, which are given by,

$$\epsilon_{c,x} = \frac{\Delta}{L} + \frac{1}{L} \int_0^L \left[\frac{1}{2} \left\{ \left(\frac{dv}{dx} \right)^2 + \left(\frac{dw}{dx} \right)^2 \right\} \right] dx \quad (6a)$$

$$\kappa_y = \frac{d^2v}{dx^2}, \quad \kappa_z = \frac{d^2w}{dx^2}, \quad \zeta = \frac{d\alpha}{dx} \quad (6b)$$

where, $\epsilon_{c,x}$, κ_y , κ_z , and ζ represent the centroidal axial strain, the curvatures about the two principal axes and the rate of twist, respectively.

In order to derive the relationship between the four generalized strains and the element freedoms, Eqs. 3, 4, and 5 is combined with Eq. 6. This leads to the expressions given below,

$$\epsilon_{c,x} = \frac{\Delta}{L} + \frac{[2(\theta_{1y}^2 + \theta_{2y}^2 + \theta_{1z}^2 + \theta_{2z}^2) - (\theta_{1y}\theta_{2y} + \theta_{1z}\theta_{2z})]}{30} \quad (7a)$$

$$\kappa_y = \left[\frac{6(\theta_{2y} + \theta_{1y})}{L^2} \right] x - \left[\frac{2(2\theta_{1y} + \theta_{2y})}{L} \right] \quad (7b)$$

$$\kappa_z = \left[\frac{6(\theta_{2z} + \theta_{1z})}{L^2} \right] x - \left[\frac{2(2\theta_{1z} + \theta_{2z})}{L} \right] \quad (7c)$$

$$\zeta = \frac{\theta_T}{L} \quad (7d)$$

The next stage is to establish the relationship between the generalized strains and the generalized stresses. Since the relationship cannot be established explicitly due to the presence of material plasticity, the integration of the virtual work equation is carried out numerically for the calculation of the element forces. Since the element can only be used to model short lengths of members as previously mentioned, the integration at two Gauss sections is employed. The location of each Gauss section is depicted in Fig. 3 and is given by,

$$x_g^1 = \frac{L}{2} \left(1 - \frac{\sqrt{3}}{3} \right), \quad x_g^2 = \frac{L}{2} \left(1 + \frac{\sqrt{3}}{3} \right) \quad (8)$$

Accordingly, the generalized strains at both Gauss sections can be represented by a matrix, \mathbf{u}_s which is determined directly from Eqs. 7 and 8. The matrix is given below,

$$\mathbf{u}_s = \begin{bmatrix} \varepsilon_{c,x} & \varepsilon_{c,x} \\ \kappa_y \left(x_g^1 \right) & \kappa_y \left(x_g^2 \right) \\ \kappa_z \left(x_g^1 \right) & \kappa_z \left(x_g^2 \right) \\ \zeta & \zeta \end{bmatrix} \quad (9)$$

Each Gauss section is divided into a number of user defined areas across which strains and stresses are monitored. If the effect of shear strains on material plasticity is ignored, only direct strains are required at the monitoring points, which are given as below,

$$e_{m,g} = \sum_{i=1}^4 d_{m,i} u_{si,g} \quad (10)$$

$$d_{m,1} = 1$$

$$d_{m,2} = -y_m \quad (11)$$

$$d_{m,3} = -z_m$$

$$d_{m,4} = 0$$

where, $e_{m,g}$ is the direct strain of monitoring point m at Gauss section g , and \mathbf{u}_{si} is the generalized strain matrix defined in Eq. 9.

In order to establish the direct stresses corresponding to the direct strains at the monitoring points, a uniaxial stress-strain relationship is employed as given in Eq. 12. In Eq. 12, f represents the stress-strain relationship of the material model used and any material model can then be applied.

$$s_{m,g} = f(e_{m,g}) \quad (12)$$

where, $s_{m,g}$ represents the material stress of monitoring point m at Gauss section g .

Whereas the bending and axial generalized stresses at Gauss section are calculated from the direct material stresses, the relation between the torsional generalized stress and strain is based on the elastic torsional rigidity constant. Thus,

$$f_{si,g} = \sum_{m=1}^n A_m d_{m,i} s_{m,g} \quad \text{for } i=1,3 \quad (13)$$

$$f_{s4,g} = G J_s u_{4,g} \quad (14)$$

where, A_m is the area of monitoring point m , $d_{m,i}$ is defined in Eq. 11 and the upper limit n in Eq. 13 represents the number of monitoring points at a Gauss section. Once the generalized stresses are determined at the two Gauss sections, the element local forces can be evaluated in terms of numerical integration of the virtual work equation. Therefore,

$$f_{ci} = \sum_{j=1}^4 \sum_{k=1}^2 T_{ci,j,k} f_{sj,k} \quad (15)$$

where T_c is a $6 \times 4 \times 2$ matrix representing weighted first derivatives of generalized strains with respect to local displacements.

The local tangent stiffness k_c can be obtained from the differentiation of Eq. 15 and is given by,

$$k_{ci,n} = k_{fi,n} + \left(\frac{2}{L}\right) \sum_{j=1}^4 \sum_{k=1}^2 \sum_{l=1}^4 T_{ci,j,k} k_{sj,l,k} T_{cn,l,k} \quad (16)$$

where k_f and k_s are determined from Eqs. 17 and 18 respectively as given below,

$$k_{f1,1} = k_{f2,2} = k_{f3,3} = k_{f4,4} = \frac{2FL}{15} \quad (17a)$$

$$k_{f1,2} = k_{f2,1} = k_{f3,4} = k_{f4,3} = -\frac{FL}{30} \quad (17b)$$

$$k_{sj,l,k} = \sum_{m=1}^n A_m d_{m,j} E_{tm,k} d_{m,l} \quad \text{for } j=1,3, \quad l=1,3 \quad (18a)$$

$$k_{s4,4,k} = GJ \quad (18b)$$

where F is the axial force and all other terms of both k_f and k_s matrices are zero. $E_{tm,k}$ in Eq. 18a represents the material tangent modulus of monitoring point m at Gauss section k and is required in the element tangent stiffness calculation needed for the iterative solution procedure. The material tangent modulus is given as below,

$$E_{tm,g} = \frac{ds_{m,g}}{de_{m,g}} = \frac{df}{d\varepsilon} (e_{m,g}) \quad (19)$$

In view of the above, a repair element is proposed for the purpose of seismic performance evaluation of reinforced concrete members and structures that have experienced prior damage. The new repair element incorporates both birth and death time and thus it can be either activated or deactivated within user-defined time intervals of interests during analysis. The time intervals of interests can freely be defined by user within the new element as birth and death time. Accordingly, the new element is capable of modeling any parts of members and structures with different time intervals of interests in both static and dynamic time-history analyses. This allows that increased or decreased response characteristics due to add or subtracted members respectively are physically reflected during the analyses. Having defined both birth and death time, the new element force and stiffness calculation is designed to start at birth time and stop at death time. The calculated new element force and stiffness at each time step are transformed to global system element level which leads to global structural system level in that time step. The incorporation of the new element in a general nonlinear procedure requires the application of three transformations between local element system to global structural system (Izzuddin 1991). The first is a geometric transformation establishing the local element displacements corresponding to a set of global displacements. The second is a transformation of the local element forces to global forces with the local forces calculated from local displacements. The two transformations establish a relationship between global forces and global displacements. The final transformation associated with local tangent stiffness matrix establishes the global tangent stiffness matrix needed for the iterative solution procedure. A detailed description regarding the three transformations is addressed in the reference (Izzuddin 1991). The general procedure for the calculation of the new element force and stiffness is schematically

summarized in a form of flow chart as shown in Fig. 4. The new repair element has been implemented into ZeusNL (Elnashai et al. 2001), which is discussed hereafter.

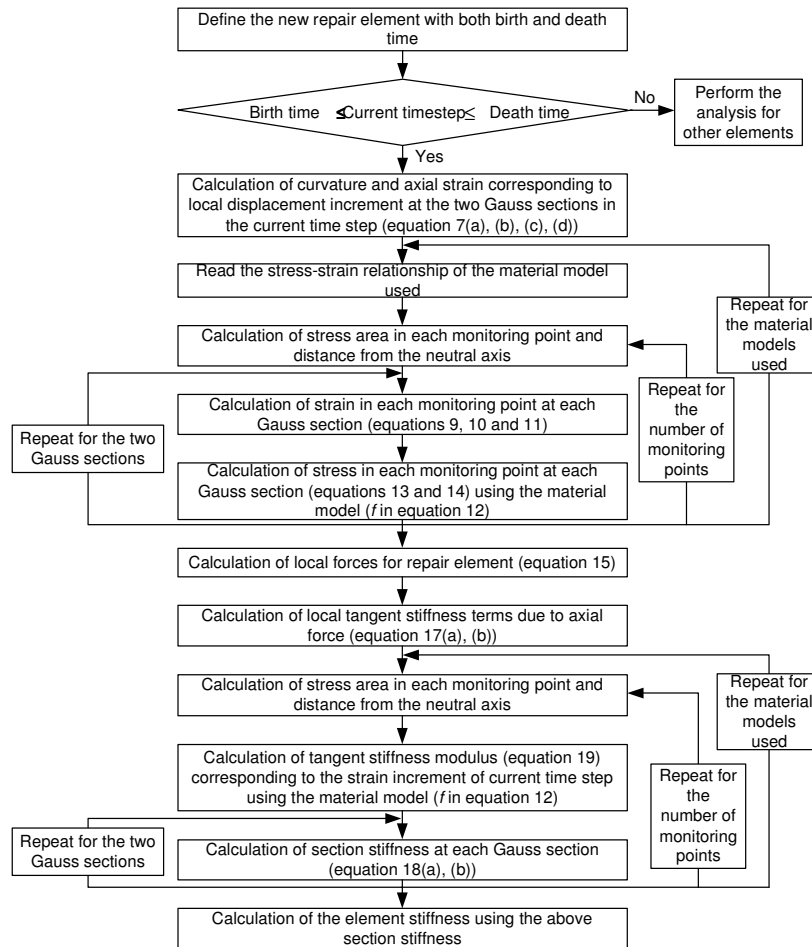


Figure 4. General procedure for the calculation of the new element force and stiffness.

Program ZeusNL

The new repair element has been implemented into the nonlinear fiber element static and dynamic analysis program ZeusNL (Elnashai et al. 2001). The program has been developed for the nonlinear analysis of two- and three-dimensional steel, reinforced concrete and composite structures, taking into account the effects of both geometric nonlinearity and material inelasticity. A detailed description of ZeusNL is available in the ZeusNL manual (Elnashai et al. 2001).

Verification of the New Element

To verify the new element, the analytical results obtained with ZeusNL incorporating the new element are compared with experimental data. The test specimens used for the comparison are reinforced concrete columns being repaired and retrofitted by steel jackets of part and full height. Six large scale reinforced concrete column tests were conducted by Chai et al. (1991) to investigate the improved performance of the columns using steel jacketing. The columns were considered to be 0.4 scale models of a prototype 1524 mm diameter bridge column, being 610 mm diameter and 3657 mm height. The test columns were repaired and retrofitted with steel jackets. Steel jackets for the columns were fabricated from 4.76 mm thick hot-rolled steel, providing a volumetric confinement ratio of 0.031. The length of steel jacket was

selected to be 1219 mm to ensure that the moment demand immediately above the jacket did not exceed 75 percent of the uncased flexural capacity. Two specimens, 1R and 3R were selected for comparative verification of the new element. Material properties and applied axial force for the selected columns, and the yield strength of steel jacket are summarized in Table 1.

Table 1. Material properties of the selected columns and yield strength of steel jacket (Chai et al. 1991).

Specimen	Test remark	Concrete strength (MPa)	Applied axial force (kN)	Longitudinal reinforcement	Transverse reinforcement	Steel jacket
				Yield strength(MPa)	Yield strength(MPa)	Yield strength(MPa)
1R	Repair	37.9	1779	313	349	308
3R	Retrofit	37.8				322

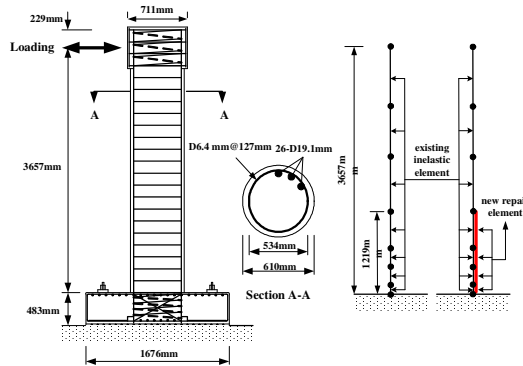


Figure 5. Dimensions, cross-section details and analytical models of test specimen (Chai et al. 1991).

Shown in Fig. 5 are column dimensions and section details of the columns tested by Chai et al. (1991). For the investigation of the column response, use is made of ZeusNL. Two different modeling approaches are utilized for the estimation of response characteristics and for the validation of the new element. Firstly, seven existing cubic inelastic elements are employed with shorter elements at the base of columns and longer elements toward their top. Such an arrangement allows potential plastic hinge zones to be accurately captured. Circular cross-section is employed to model the column cross-section across which 200 monitoring points are defined to account precisely for the inelastic response of the columns. Secondly, the new elements are employed for the column lengths of 1219 mm being repaired or retrofitted by steel jacket and added to the first model, as depicted in Fig. 5. Circular steel hollow section with inner diameter corresponding to the column diameter is employed for the new elements. The new elements are modeled to activate only during the second loading history, which in turn the new elements are deactivated during the first loading history. This allows increased characteristics due to repair or retrofitting by steel jackets to be realistically reflected to the column response experienced the first loading history.

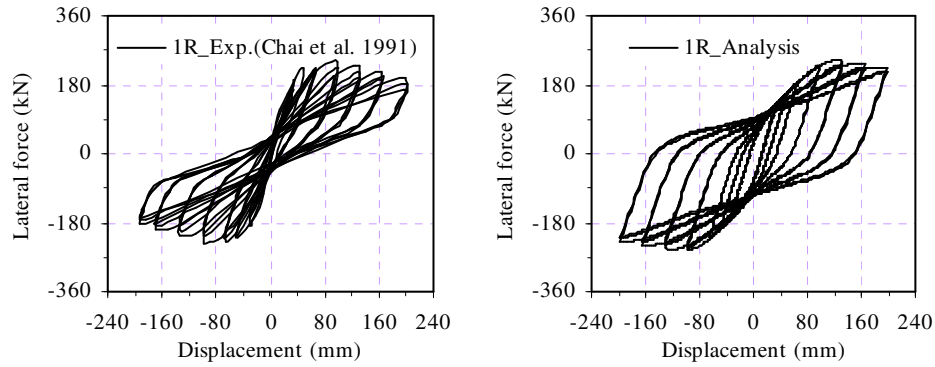


Figure 6. Comparison of hysteretic response for repaired specimen 1R.

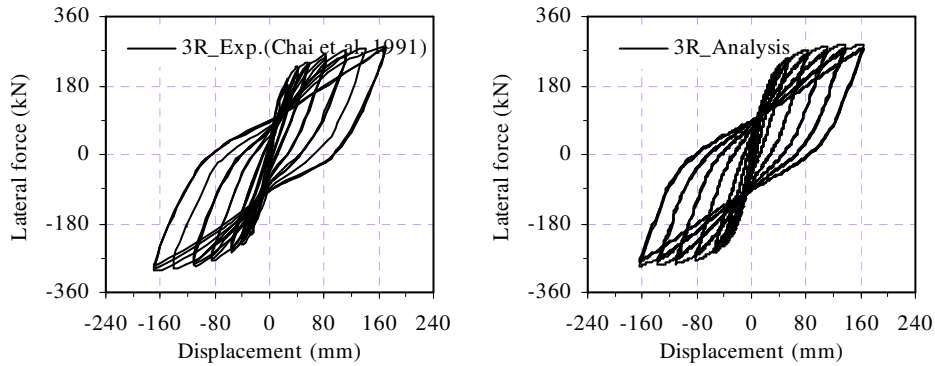


Figure 7. Comparison of hysteretic response for retrofitted specimen 3R.

Fig. 6 shows comparison of load-displacement hysteretic response for specimen 1R repaired by steel jacket. Experimental results show the strength degradation as ductility is increased and analytical results incorporating the new element exhibit similar trend. However, the analytical results overestimate the energy dissipation capacity and hence pinching effect in comparison with the experimental results. This may be attributed to bond failure and shear failure in the column-footing interface observed in the experiment, which are not taken into account in the analysis. Shown in Fig. 7 is comparison of load-displacement hysteretic response for retrofitted specimen 3R. The experimental results show no strength degradation and hence stable response as ductility is increased. The analytical predictions incorporating the new element display similar trend and is well-correlated with the experimental results in overall inelastic response.

Another comparative study has been conducted for reinforced concrete column tests. Priestley et al. (1994a, b) carried out eight circular column tests in order to establish the effectiveness of full height steel jackets as a retrofit measure. Columns were designed at 0.4 scale models of a prototype and the test set up was designed to subject the columns to axial loading and cyclic shear forces under reversed curvature, with the point of contra-flexure occurring at the column mid-height. Section dimensions and loading conditions are shown in Fig. 8. Two retrofitted specimens, C2R and C6R were selected as representative cases. Material properties and applied axial forces for the chosen columns are provided in Table 2, together with steel jacket details.

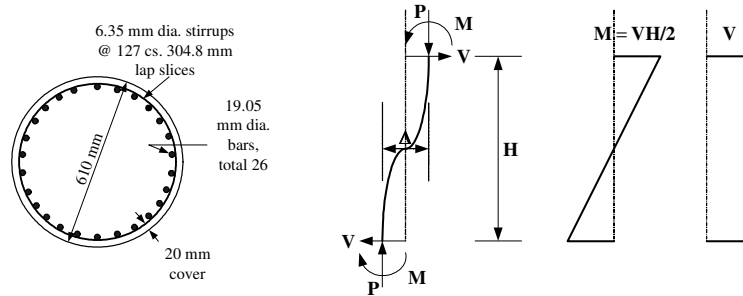


Figure 8. Cross-section details and loading conditions (Priestley et al. 1994a).

Table 2. Material properties and applied axial force for the selected columns (Priestley et al. 1994a).

Specimen	Aspect ratio M/VD	Concrete strength (MPa)	Applied axial force (kN)	Longitudinal reinforcement	Transverse reinforcement	Steel jacket	
				Yield strength(MPa)	Yield strength(MPa)	Yield strength (MPa)	Thickness (mm)
C2R	2.0	34.0	598.5	324	359	348	4.76
C6R	2.0	40.0		469	324	286	3.18

ZeusNL is again utilized for the comparative studies. As in the case of the former analytical modeling approaches, existing cubic inelastic elements are employed for as-built columns, while the new elements are employed for the full height of columns to reflect the steel jacket retrofitting using circular steel hollow section with inner diameter corresponding to the column diameter. Since the experimental study is dealing with retrofitting, the new repair elements employed are activating from the beginning of loading history. In the analytical modeling of columns, shorter elements at the top and base of columns and longer elements toward their centers are employed to accurately capture the potential plastic hinge zones at the two critical regions of columns. Other assumptions with regard to material models, etc. are the same as those used for the former comparative studies. Fig. 9 shows comparison of hysteretic response for specimen C2R. Experimental results exhibit stable and ductile response and thus no strength and stiffness degradation is observed. The analytical results also shows a similar response in terms of both strength and stiffness. Nevertheless, there is a slight difference in energy dissipation capacity. This can be attributed to the fact that the aspect ratio of the columns is two and thus the response of columns can be affected by shear which is not taken into account in the current analysis. Notwithstanding, overall response between experiment and analysis is reasonably correlated. Shown in Fig. 10 is comparison of hysteretic response for specimen C6R. Similar response as for the case of C2R is exhibited.

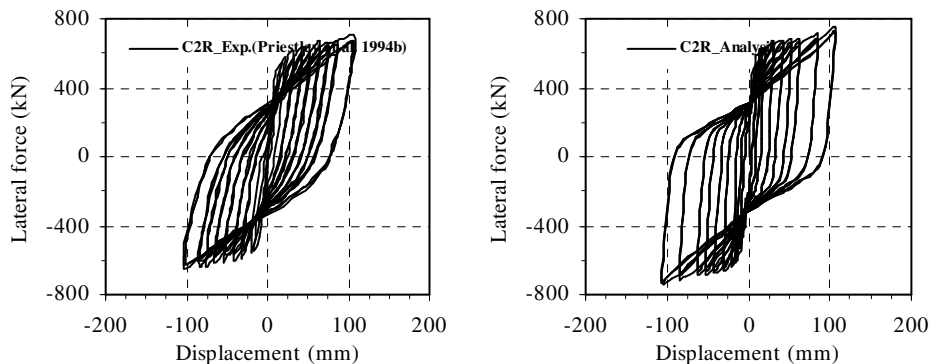


Figure 9. Comparison of hysteretic response for specimen C2R.

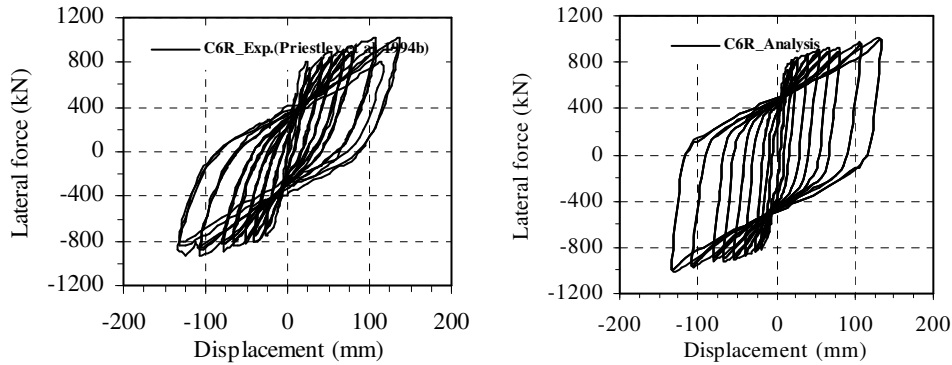


Figure 10. Comparison of hysteretic response for specimen C6R.

In all, the verification examples above demonstrate that the new element proposed in this paper gives reasonably good predictions of column response being repaired and retrofitted by steel jackets. This indicates that the current development is promising for the seismic assessment of reinforced concrete column members, being repaired and retrofitted by steel jacket after experiencing a prior earthquake damage. There is certainly room for more improvements as various material models, such as FRP and GFRP become available in ZeusNL.

Conclusions

Repair element having both birth and death time has been suggested and implemented in the nonlinear static and dynamic analysis program ZeusNL. The new repair element can be simulated in static and dynamic time-history analysis and activated within the user-defined time intervals of interests. Verification of the new element was achieved in terms of comparisons with reinforced concrete columns being repaired and retrofitted subjected to cyclic load reversals. The comparison showed that the analytical predictions incorporating the new element gave a reasonably good correlation with experimental results in terms of both strength and stiffness. In short, the present development allows the increased characteristics due to repair and retrofitting to be realistically reflected on the response of members and structures experienced prior damage and thus is expected to give a feasible information with regard to the seismic upgrading. Meanwhile, the current study is limited for RC members, particularly columns and piers repaired or retrofitted by steel jacket. Accordingly, more valuable improvements and verifications of the new element are expected when various material models, such as FRP and GFRP become available in ZeusNL.

Acknowledgments

The work presented in this paper was funded by the Center for Concrete Corea (05-CCT-D11), supported by Korea Institute of Construction and Transportation Technology Evaluation and Planning (KICTTEP) under the Ministry of Construction and Transportation (MOCT).

References

- Chai, Y.H., Priestley, M.J.N. and Seible, F., 1991. Seismic retrofit of circular bridge columns for enhanced flexural performance, *ACI Structural Journal*, 88 (5), 572-584.
- Elnashai, A.S., Papanikolaou, V. and Lee, D.H., 2001. ZeusNL-A program for inelastic dynamic analysis of structures, *Mid-America Earthquake Center, University of Illinois at Urbana-Champaign, USA*.
- Izzuddin, B.A., 1991. Nonlinear dynamic analysis of framed structures, *PhD thesis, Imperial College, London*.

- Izzuddin, B.A. and Elnashai, A.S., 1993a. Adaptive space frame analysis Part I: a plastic hinge approach, *Proceedings of Institution of Civil Engineers Structures & Buildings*, 99, 303-316.
- Izzuddin, B.A. and Elnashai, A.S., 1993b. Adaptive space frame analysis Part II: a distributed plasticity approach, *Proceedings of Institution of Civil Engineers Structures & Buildings*, 99, 317-326.
- Priestley, M.J.N., Seible, F., Xiao, Y. and Verma, R., 1994a. Steel jacket retrofitting of reinforced concrete bridge columns for enhanced shear strength-Part1: theoretical considerations and test design, *ACI Structural Journal*, 91 (5), 394-405.
- Priestley, M.J.N., Seible, F., Xiao, Y. and Verma, R., 1994b. Steel jacket retrofitting of reinforced concrete bridge columns for enhanced shear strength-Part2: test results and comparison with theory, *ACI Structural Journal*, 91 (5), 537-551.
- Sucuoglu, H., 2002. Engineering characteristics of the near-field strong motions from the 1999 Kocaeli and Duzce earthquakes in Turkey, *Journal of Seismology*, 6 (3), 347-355.
- Uckan, E., Owen, V.A. and Erdik, M., 2002. A study of the response of the Mustafa Inan viaduct to the Kocaeli earthquake, *Bulletin of the Seismological Society of America*, 92 (1), 483-98.